

Fluvial architecture of the Burro Canyon Formation using UAV-based photogrammetry and outcrop-based modeling: implications for reservoir performance, Rattlesnake Canyon, southwestern Piceance Basin, Colorado

Kelsey D. Lewis¹, Matthew J. Pranter¹, Zulfiquar A. Reza² and Rex D. Cole³

¹ConocoPhillips School of Geology and Geophysics, University of Oklahoma, Norman, OK 73019

²Mewbourne School of Petroleum and Geological Engineering, University of Oklahoma, Norman, OK 73019

³Department of Physical and Environmental Sciences, Colorado Mesa University, Grand Junction, CO 81501

ABSTRACT

The stratigraphic variability of fluvial architectural elements and their internal lithological and petrophysical heterogeneity influence static connectivity and fluid flow. Analysis of the fluvial architecture and facies heterogeneity of the Lower Cretaceous Burro Canyon Formation provides insight regarding their impact on reservoir performance. The Burro Canyon Formation as exposed in Rattlesnake Canyon, Colorado, forms stacked amalgamated and semi-amalgamated channel complexes that consist of amalgamated and isolated fluvial-bar channel deposits and floodplain fines, and represents a perennial, braided-fluvial system. Detailed two- (2-D) and three-dimensional (3-D) static and dynamic reservoir models are constrained using stratigraphic measured sections, outcrop gamma-ray measurements, and Unmanned Aerial Vehicle (UAV)-based photogrammetry. Resulting breakthrough time and sweep efficiency suggest subsurface reservoir performance is most effective perpendicular to paleoflow direction in amalgamated channels. Perpendicular to paleoflow, breakthrough time is 9% shorter than parallel to the paleoflow and sweep efficiency is, on average, 16% greater due to greater sandstone connectivity in this orientation. Variability of preserved channels and lateral pitchouts results in lower recovery efficiency. Facies heterogeneity can account for 50% variation in breakthrough time and slightly lower recovery efficiency (5%). Cemented conglomerates that form channel lags above basal scour surfaces can also create fluid-flow barriers that increase breakthrough time and decrease sweep efficiency (25%) and recovery efficiency (22%).

INTRODUCTION

The stratigraphic variability of fluvial deposits and their internal lithofacies and petrophysical heterogeneity influence sandstone-body connectivity and reservoir performance. At the reservoir scale, architectural elements and their stacking

patterns create large-scale heterogeneity that influences reservoir productivity (e.g., Pranter et al., 2007, 2009; Villamizar et al., 2015). Lithofacies associations and their associated reservoir properties create internal heterogeneity within fluvial deposits that also impact fluid-flow (e.g., Pranter et al., 2007; Massart et al., 2016). Understanding the impact of different scales of fluvial heterogeneity on reservoir performance (e.g., sweep efficiency, recovery efficiency, breakthrough time of injected fluids at producing wells) is useful when characterizing and developing these types of reservoirs. To further explore how these types of sedimentological heterogeneities impact reservoir performance, well-exposed fluvial outcrop analogs of the Lower Cretaceous Burro Canyon Formation in Colorado are used as an example.

The Piceance Basin resides in an area once occupied by a much larger Rocky Mountain Foreland Basin formed by the Sevier Orogeny (c. 140-50 Ma) (Johnson and Flores, 2003). Early Cretaceous clastic sediments deposited in the Rocky Mountain Foreland Basin were transported from the Sevier fold-thrust belt eastward and northeast and deposited in the distal portion of the basin (Johnson, 1989; DeCelles, 2004). Deposition of the clastic sediments took place in a series of pulses due to orogenic movements from Aptian to Albian times. In the Late Cretaceous, the Laramide Orogeny caused structural deformation and formation of the modern day Piceance Basin (DeCelles, 2004).

The Lower Cretaceous Burro Canyon Formation is exposed in numerous canyons along the Gunnison River in the southwestern Piceance Basin, northwestern Colorado (Figure 1), and forms minor sandstone reservoirs within the basin (Young, 1975). The Burro Canyon Formation represents braided to meandering river deposits that formed in a coastal-plain setting (Stokes, 1952; Kirkland et al.,

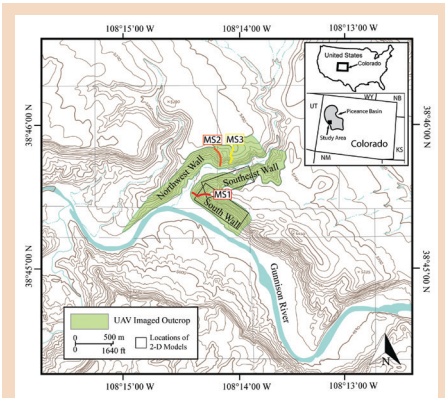


Figure 1: Rattlesnake Canyon study area.
MS=measured section.

1999; Kirkland and Madsen, 2007; Currie et al., 2008; Cole and Moore, 2012). The Burro Canyon Formation unconformably overlies the Upper Jurassic Morrison Formation and is unconformably overlain by the Cretaceous Dakota Formation (Young, 1975) (Figure 2). Burro Canyon Formation lithofacies primarily consists of: 1) fine- to coarse-grained sandstone and conglomerate, 2) sandy granule-pebble conglomerate, and 3) green calcareous mudrock.

This study further establishes the depositional environment and stratigraphic architecture of the Burro Canyon Formation. The significance of the stratigraphic architecture and the different scales of fluvial sedimentological heterogeneity on reservoir performance is explored using the well-exposed outcrops of the Burro Canyon Formation in Rattlesnake Canyon, Colorado. Additional details are explained in Lewis (2018).

METHODOLOGY

The Burro Canyon Formation is well exposed on three sides of Rattlesnake Canyon. Outcrop orientations provide perspectives that are both sub-perpendicular and parallel to the paleoflow direction. Outcrops were analyzed through three measured sections (MS-1 to MS-3; total length ~360 ft, ~110 m) for lithology, grain-size, sedimentary structures, bounding surfaces, and deposit width, thickness, and orientation. Outcrop samples for petrographic analysis of thin

sections were obtained at significant lithological changes along the traverses. Paleocurrent measurements (N=124, M=58°) based on the dip and azimuth of cross-stratification were acquired for multiple stratigraphic levels. Using a DJI Phantom 3 drone, high-resolution images were systematically acquired at three different distances from the outcrop (10-100 ft; 3-30 m). This was done to capture large-scale features such as channel geometries and architectural elements and small-scale features such as sedimentary structures. The georeferenced images were used to create a digital 3-D point-cloud model of Rattlesnake Canyon. Vertical lithofacies logs for 127 pseudo sections were created along the outcrops using a 30-ft (10-m) lateral spacing and 0.33 ft (0.1 m) vertical sample increment. The pseudo wells capture the bounding surfaces and lithofacies as exposed in Rattlesnake Canyon. The lithofacies logs and surfaces were used to create stratigraphic zones for geologic (static) models and to constrain lithofacies models.

Two 2-D model grids are oriented parallel to paleoflow, and two 2-D model grids are oriented perpendicular to paleoflow (Figure 3). One 3-D

model grid was created. Both 2-D and 3-D grids have cell dimensions that are 3 ft x 3 ft x 0.3ft (1 m x 1 m x 0.1 m). The 2-D and 3-D models include the stratigraphic interval from the base of the uppermost channel in the Morrison Formation to the base of the Dakota Formation; thus, incorporating the entire Burro Canyon interval. For each paleoflow orientation, the stratigraphic zones associated with the two 2-D grids reflect different levels of stratigraphic detail. The first grid has zones defined for each isolated-sandstone body (e.g., fluvial channel fill; Patterson et al., 2012) and amalgamated-sandstone body encompassed in floodplain mudstone (herein referred to as the sandstone-body model); note that smaller scale zones are not defined within the amalgamated-sandstone bodies. The second grid includes more stratigraphic detail and zones are defined for each channel fill (herein referred to as the channel-fill model; Figure 3). The 3-D model grid includes the same stratigraphic details and zones as defined for the 2-D channel-fill model. For the 3-D model, zones (channel fills) were mapped in three dimensions by using projected stratigraphic surfaces

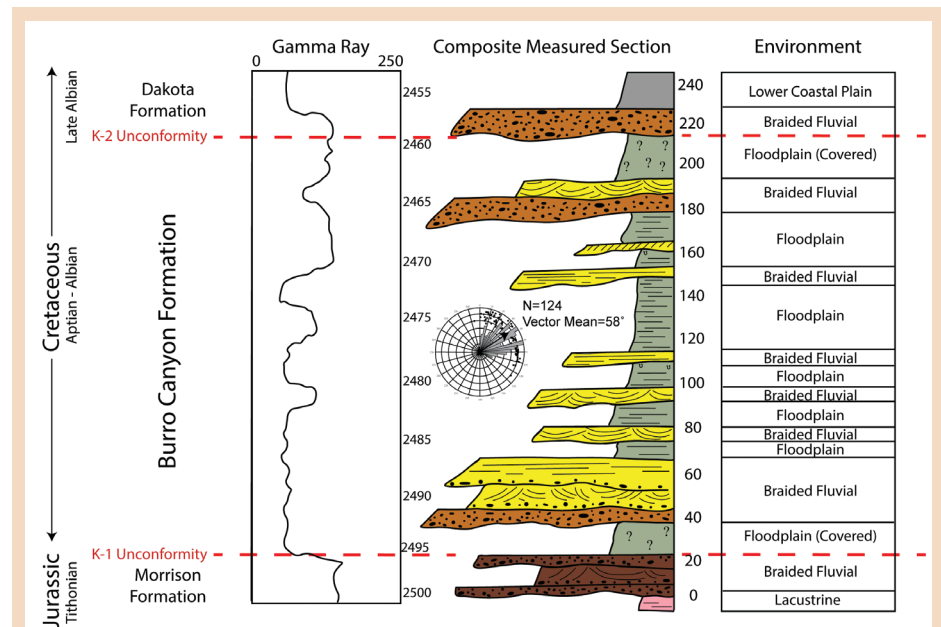


Figure 2: Composite measured section from Rattlesnake Canyon of the uppermost Morrison Formation Burro Canyon Formation, and lower Dakota Formation. Gamma-ray log from Mitchell Energy 8-1 Federal well (approximately 30 miles away). Includes rose diagram of Burro Canyon Formation paleocurrent measurements (N=124, vector mean=58 degrees).

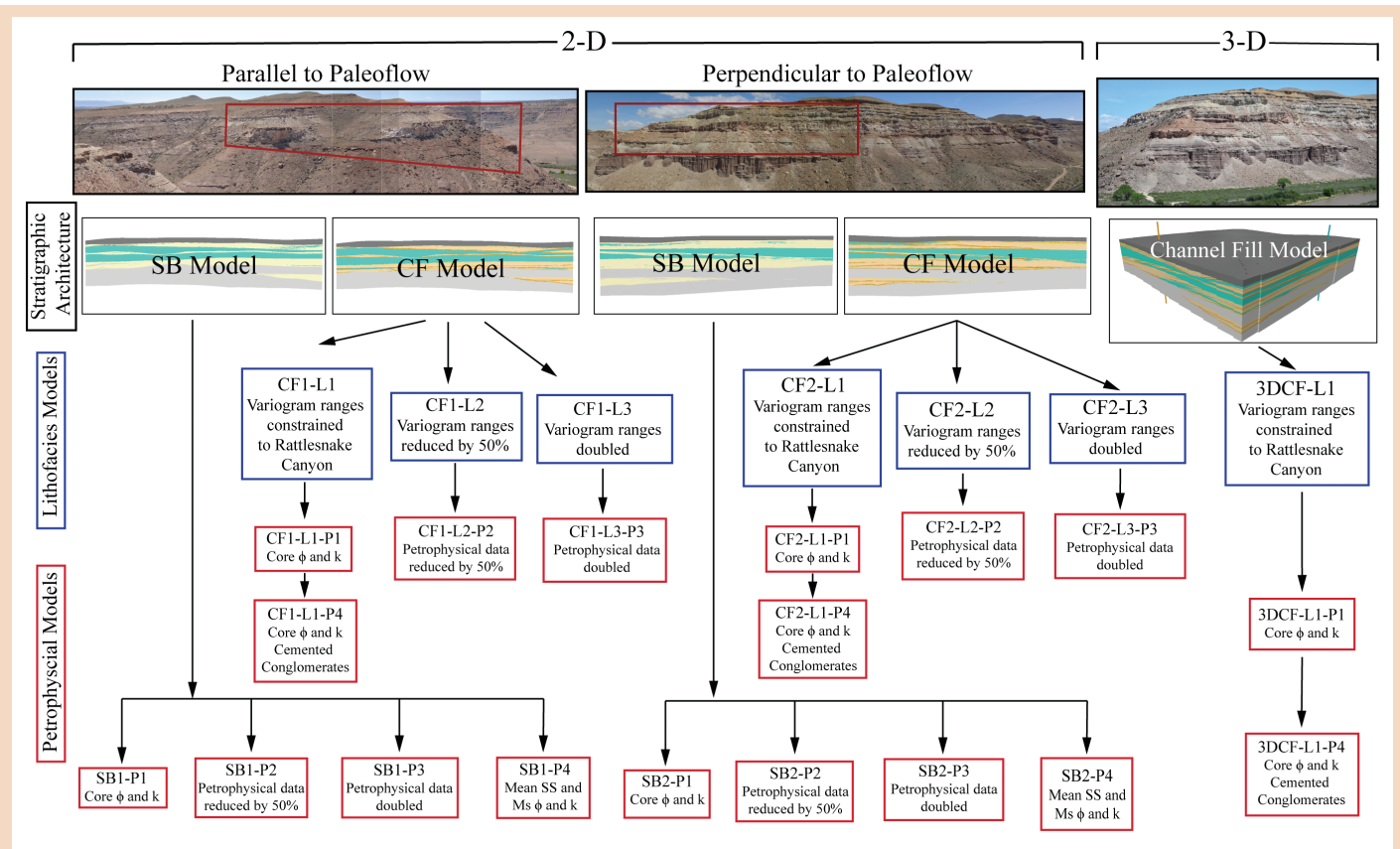


Figure 3: Diagram depicting model scenarios created using Burro Canyon Formation data from Rattlesnake canyon. Two-dimensional models have been oriented parallel and perpendicular to paleoflow directions. Within each 2-D orientation is a Sandstone Body (SB) model and a Channel-Fill (CF) model. SB models contain sandstone bodies along the outcrop and grouped together, individual channel fills and scour surfaces are not defined within this model. Within the SB model, four petrophysical scenarios are defined in each direction. CF models contain individually defined channel-fill deposits and incorporates zones of mudstone that may be present in between these channel fills. CF models are broken into three lithofacies models with associated petrophysical models. The 3-D model is classified as a CF model as it contains individually defined channel fill deposits; variogram ranges for lateral extent of lithofacies found in outcrop observations. The 3-D lithofacies model is used in two petrophysical models.

defined from the 3-D digital outcrop model and 151 pseudo wells. As with the 2-D channel-fill model, the channel fills that form each zone exist as both isolated sandstone bodies and more complex amalgamated sandstone bodies composed of stacked channel fills. Additional details are provided in Lewis (2018).

For each paleoflow orientation, eight different outcrop-based lithofacies were modeled within individual sandstone bodies of the channel-fill models using sequential-indicator simulation with the following data and constraints: (1) channel-fill models (lithofacies were modeled within each channel fill); (2) lithofacies logs for pseudo wells (N=38); and (3) variogram parameters. Variogram inputs were estimated from outcrop measurements of lateral and vertical lithofacies continuity derived

from measured sections, pseudo well lithofacies logs, and the 3-D digital outcrop models. Three different lithofacies model scenarios were produced by using different horizontal variogram ranges to explore the impact of lateral lithofacies continuity on various reservoir performance metrics. A high-resolution 3-D lithofacies model was also constructed using sequential-indicator simulation.

For both paleoflow orientations, porosity and permeability models were generated using the sandstone-body models and channel-fill lithofacies models as constraints (Figure 3). High-resolution porosity and permeability models were created by either assigning mean values or mapped using sequential-Gaussian simulation (SGS) with the following data and constraints: (1) sandstone-body models or channel-

fill lithofacies models; (2) triangular porosity and permeability distributions for sandstone and mudstone, or average values of porosity and permeability, or triangular porosity and permeability distributions for each lithofacies (core data from the Mitchell Energy Federal 8-1 well), and (3) variogram parameters.

For each sandstone-body model (for both orientations), four porosity and permeability model scenarios were generated (Figure 3). For the first model scenarios, triangular porosity and permeability distributions were used with SGS to map these properties within sandstone and mudstone model lithologies. For the second and third model scenarios, the porosity and permeability values were reduced by 50% and doubled, respectively, to test the impact on reservoir performance.

For the fourth model scenario a, more simplistic model was produced as mean values for sandstone and mudstone porosity and permeability were assigned to the corresponding model lithologies.

For each of the six channel-fill lithofacies models, a corresponding porosity and permeability model was generated (Figure 3). For the first porosity and permeability models, triangular porosity and permeability distributions for each lithofacies were used with SGS to map the properties. Second and third model scenarios, porosity and permeability values were reduced by 50% and doubled, respectively. Two additional porosity and permeability models were generated in each orientation that were conditioned to the first channel-fill lithofacies models. However, the final two models assume that the conglomerates are significantly cemented; therefore, the corresponding porosity and permeability values were reduced to a range of 0–8% (mean = 4%) and 0.001–0.5 mD (mean = 0.02), respectively, similar to previously documented cemented braided-fluvial deposits (Clarke, 1979; Cant and Eth, 1984).

Two 3-D porosity and permeability model scenarios were generated with sequential-Gaussian simulation using the 3-D lithofacies model as a constraint (Figure 3). The first model uses the same porosity and permeability histogram and variograms as with the first 2-D channel-fill porosity and permeability models. Like the 2-D cemented conglomerate scenario, a second set of porosity and permeability models were generated that assume the conglomerates are significantly cemented.

Two-phase oil-water fluid-flow simulations are performed using single injector and production wells with commercial reservoir simulation software. Models were constructed at reservoir conditions. Simulations for 2-D and 3-D models are each run for 100 and 120 years, respectively, to ensure water breakthrough. Simulations are evaluated in terms

of 1) breakthrough time (BTT), 2) volumetric sweep efficiency (SE) at BTT, 3) recovery efficiency (RE) at BTT and at 100 years, and 4) cumulative production of oil, gas, and water at 100 years. For the swept volume calculation, cells were considered with water saturation greater than connate water saturation. The sum of the volume of these detected cells divided by the total cell volume of the model cells determines the SE.

RESULTS

The Burro Canyon Formation consists of alternating lenticular beds of fine- to medium-grained sandstones and conglomerates interbedded with gray-green mudstones. In Rattlesnake Canyon, the Burro Canyon Formation consists of eight lithofacies: (1) granule-pebble conglomerate; (2) trough cross-bedded sandstone; (3) chert-rich sandstone; (4) planar-laminated sandstone; (5) structureless sandstone; (6) low-angle planar-laminated sandstone; (7) fissile gray-black mudstone; and (8) gray-green mudstone. The Burro Canyon Formation contains isolated

to amalgamated sandstone bodies that range from 3.7–33.8 ft (1.1–10.3 m) in thickness and often exhibit an upward-fining grain-size profile. The sandstones are generally conglomeratic at the base and beds thin upward into a fine- to medium-grained sandstone. Sandstone bodies are bounded at the base by sharp scour surfaces and are commonly amalgamated.

The Burro Canyon Formation represents a single depositional sequence that is composed of a lower amalgamated channel complex and overlying semi-amalgamated channel complex and consist of four key architectural elements (facies associations) that stack to form a depositional sequence: (1) channel complex (amalgamated, semi-amalgamated), (2) amalgamated fluvial-bar channel-fill deposits, (3) isolated fluvial-bar channel-fill deposits, and (4) floodplain fines (Figure 4). The largest architectural element, amalgamated channel complexes, consist of channel-fill elements that are vertically stacked and overlain by a mudstone-dominated interval of semi-amalgamated channel complex

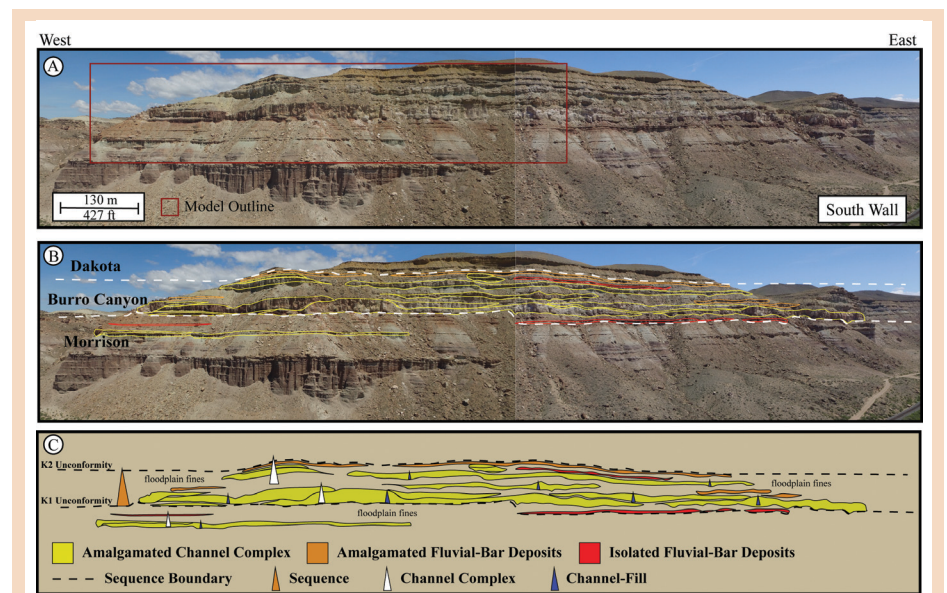


Figure 4: Photomosaic of architectural elements and hierarchical elements along the South Wall of Rattlesnake Canyon associated with those defined by Patterson et al., 2012 and Sprague et al., 2002. Facies associations are outlined in yellow, orange and red. Unfilled areas represent floodplain fines architectural element. A single sequence represents the entire deposition of the Burro Canyon and contains two channel complexes. The first being an amalgamated channel complex towards the base of the sequence, topped by a semi-amalgamated channel complex near the top of the sequence.

The **Sedimentary** Record

elements. The amalgamated channel complex is sandstone-prone and possesses an erosional base interpreted as a sequence boundary. Amalgamated fluvial-bar channel-fill deposits form sandstone beds with an upward-fining nature and are horizontal-planar laminated to low-angle planar-laminated lithofacies. Amalgamated

fluvial-bar channel-fill deposits are encased in floodplain mudstones and are less extensive than amalgamated channel complexes. Amalgamated fluvial bars range from 4 to 35 ft (1.2 to 10.5 m) in thickness with width-to-thickness ratios range from 5:1 – 155:1. Isolated fluvial-bar channel-fill deposits are fining-upward sandstone successions

encased in floodplain mudstones that together form a semi-amalgamated channel complex. Low-angle planar laminations and minor horizontal-planar laminations are common in these architectural elements and mudstone rip-up clasts occur irregularly throughout the deposits. Isolated fluvial-bar deposits are relatively thin and laterally continuous, averaging 2 ft (0.6 m) in thickness. The gray-green mudstones are interpreted as alluvial floodplain (floodplain fines) and are indicative of the Burro Canyon Formation throughout the Piceance Basin (Currie et al., 2008; McPherson et al., 2008). Floodplain deposits encase channel deposits, have no discrete boundaries, and are considered as non-reservoir rocks in this study (Figure 5).

Comparison of breakthrough time (BTT), sweep efficiency (SE) at BTT and 100 years, recovery efficiency (RE), and cumulative production of oil and water illustrates the effects of reservoir heterogeneity on fluid flow. Reservoir heterogeneity has a significant impact upon BTT. As a reference case, in general sandstone-body models with assigned mean values for porosity and permeability have the longest BTT as they exhibit more “piston-like” displacement. In contrast, petrophysically heterogeneous sandstone-body and channel-fill models that are constrained by outcrop-based spatial statistics (variogram ranges) produce, on average, 43% and 46% shorter BTT, respectively, as compared to petrophysically homogeneous sandstone-body models. On average, due to greater sandstone connectivity, models oriented perpendicular to paleoflow experience a 9% shorter BTT than models oriented parallel to paleoflow. For both orientations, the homogenous sandstone-body models produce the longest BTT. In general, BTT is less sensitive to changes in variogram range (only 1% difference). Incorporating cemented conglomerates, which account for 21% of lithofacies, has a more significant impact on BTT causing, on average, 9% shorter BTT for 2-D models (both orientations) and

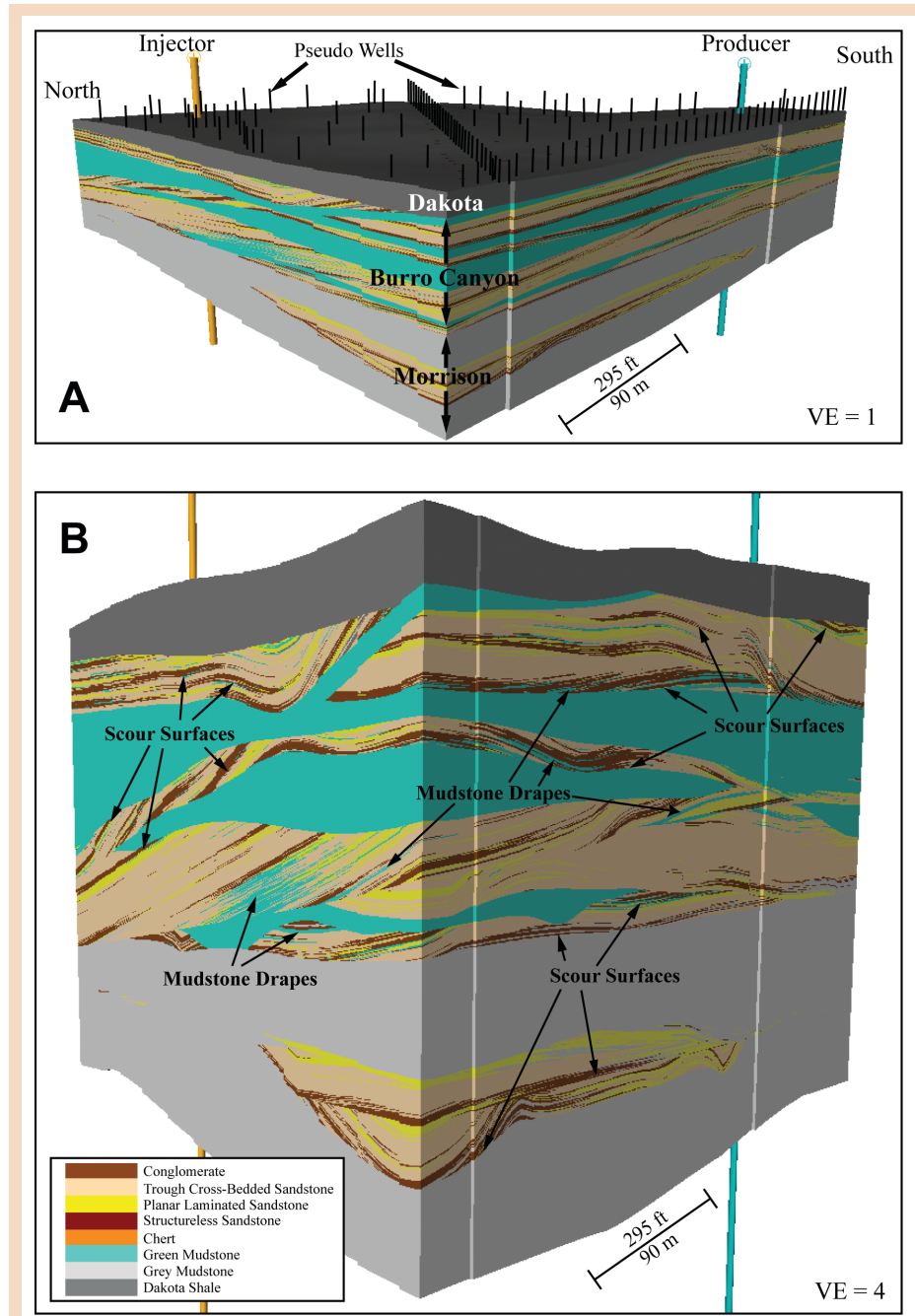


Figure 5: A) Three-dimensional static geologic model of Rattlesnake Canyon with no vertical exaggeration (VE=1). Black lines indicate position of 151 pseudo wells created to constrain geologic model. B) Vertically exaggerated (VE=4) three-dimensional static geologic model of Rattlesnake Canyon. Vertical exaggeration reveals scour surfaces and internal mud drapes within individual channel complexes of the Burro Canyon Formation. Basal conglomerates can be seen dividing up individual scour surfaces within channel complexes showing locations of individual channels.

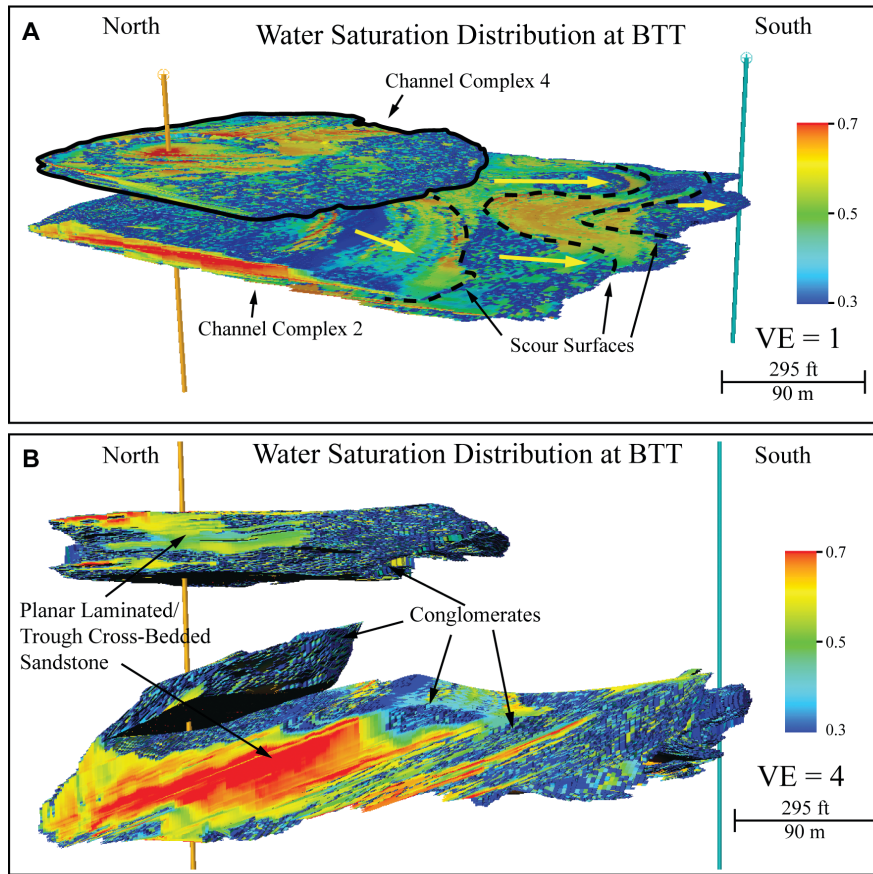


Figure 6: Three-dimensional dynamic reservoir model for 3DCF-L1-P1 model. This three-dimensional reservoir model was simulated through breakthrough time. Resulting water saturation model is shown depicting reservoir saturation at breakthrough time. A) Amalgamated channel complex shows the most efficient fluid flow pathways for production. Individual channel scours and flow pathways can be observed in this channel complex. B) When the water saturation distribution is magnified (VE=4) fluid-flow pathways can be observed. Water saturation is largely confined to the main channels of the reservoir in the trough cross-bedded and planar laminated sandstones. Low water saturation is observed in the conglomeratic intervals of the formation.

32% short BTT for 3-D models.

Two-dimensional models orientated perpendicular to paleoflow exhibit 16% higher SE than those oriented parallel to paleoflow. For 2-D models with cemented conglomerates, SE is 26% lower perpendicular to paleoflow and 23% lower parallel to paleoflow. The base-case 3-D model exhibits an average SE of 32% (Figure 6). Cemented conglomerates in 3-D produced 28% higher SE than in the base-case 3-D model.

RE for oil is the ratio of cumulative oil volume produced for a specified time period divided by the oil volume initially in place. RE is calculated at BTT and also at the end of the 100-year simulation period to insure full BTT of 3-D models. RE is sensitive to

similar parameters as SE. Perpendicular to paleoflow, 2-D models on average, result in 14% higher RE than parallel to paleoflow. RE for cemented channel-fill models, perpendicular and parallel to paleoflow, are 15% and 13% lower, respectively, than channel-fill models that incorporate outcrop-derived spatial statistics. RE is less sensitive to changes in variogram range. For 3D models, RE is 22% lower with the cemented conglomerates as compared to the 3-D base-case model. On average, models perpendicular to paleoflow produced 23% more oil than those parallel to paleoflow. Variations in variogram range produced limited change in the cumulative oil produced at 100 years. For models with short ranges, a 4% increase in cumulative oil volume

produced is observed as compared to models with outcrop-based ranges. For models with long ranges, a 6% decrease in cumulative oil volume produced is observed as compared to the models with outcrop-based ranges. Shorter variogram ranges show an increase in cumulative oil volume produced; however additional simulations are needed to confirm the magnitude of the increase.

Petrophysically homogeneous sandstone-body models exhibit SE and RE at BTT that are 37% and 27% greater, respectively, than heterogeneous channel-fill models that are constrained by petrophysical properties based on outcrop spatial statistics. Incorporating and honoring the petrophysical properties of each facies rather than having a wide distribution across facies decreases both SE and RE. Heterogeneous channel-fill models exhibit, on average, 21% lower SE at BTT and 5% lower RE at BTT than relatively homogeneous sandstone-body models. For the different heterogeneous channel-fill models, changes in the variogram range had limited effect on SE (1%) or RE (1%). Incorporating cemented conglomerates reduced cumulative oil production by 49% as compared to channel-fill models with non-cemented conglomerates. Intuitively, cement forms barriers that create tortuous fluid-flow pathways in the reservoir.

DISCUSSION

Characterization and modeling of fluvial reservoirs are challenging because fluvial reservoirs are heterogeneous at different scales as related to the stratigraphic framework, architectural elements, and lithofacies (Jackson, 1977; Miall, 1988; Willis, 1989; Sharp et al., 2003). Fluvial reservoir connectivity varies at the field scale owing to the stratigraphic variability in sandstone-body stacking patterns (e.g., Robinson and McCabe, 1997; Willis, 2007; Pranter et al., 2009; Smith et al., 2009), and lithofacies associations (architectural elements) exhibit internal heterogeneity that impacts fluid flow

(e.g., Pranter et al., 2007; Fustic et al. 2011; Hubbard, et al., 2011; Labrecque, et al., 2011).

The results of this outcrop-analog study further illustrate how channel architecture and lithofacies heterogeneity of a fluvial reservoir can act as baffles or barriers to fluid flow within a reservoir and impact the spatial distribution of petrophysical properties, fluid-flow behavior, and reservoir performance in terms of BTT, SE, and RE. The representation of stratigraphic and lithofacies architecture and petrophysical properties within modeled fluvial deposits is important depending on the degree of heterogeneity.

Given the geometries and spatial variability of Burro Canyon Formation architectural elements and the relatively low net-to-gross ratio, a high well density is required to effectively deplete the reservoirs. Channel-fill reservoir bodies contain fine-scale lithologic heterogeneity and directional permeability associated with trough cross-bedded sandstone, planar-laminated sandstone, conglomeratic beds, and other facies that influence fluid movement throughout the reservoir. Given the connectivity ratios of the architectural elements present in Rattlesnake Canyon, sandstone connectivity and channel amalgamation is greatest perpendicular to paleoflow direction, indicating swifter BTT. This result indicates when producing a braided-fluvial reservoir with similar amalgamated and semi-amalgamated channel complexes, it would be favorable to align production-injection well pairs such that displaced fluids flow perpendicular to paleoflow direction to achieve higher SE and RE. Because upward-fining grain-size trends can partially compartmentalize the reservoir vertically and reduce SE, deviated wells might be preferred depending on the magnitude of grain-size variability. However, if lithological variability exists and vertical wells are used, producer-injector well pairs should be aligned perpendicular to the paleoflow direction to maximize SE.

CONCLUSIONS

The Burro Canyon Formation as exposed in Rattlesnake Canyon, Colorado, forms stacked amalgamated and semi-amalgamated channel complexes that consist of amalgamated and isolated fluvial-bar channel deposits and floodplain fines, and represents a low-to-moderate sinuosity, braided-fluvial system. Detailed two- and three-dimensional static and dynamic models of the deposits that are constrained to stratigraphic measured sections, outcrop gamma-ray measurements, and UAV-based (Unmanned Aerial Vehicle-based) photogrammetry illustrate the impact of stratigraphic, facies, and petrophysical heterogeneity on reservoir performance. Resulting BTT and SE suggest subsurface reservoir performance is most effective perpendicular to paleoflow direction in amalgamated channels. Perpendicular to paleoflow, BTT is 9% shorter than parallel to the paleoflow and SE is, on average, 16% greater due to greater sandstone connectivity in this orientation. Variability of preserved channels, scour surfaces, and lateral pitchouts results in lower RE. Facies heterogeneity can account for 50% variation in BTT and lower RE (5%). Cemented conglomerates that form channel lags above basal scour surfaces can also create fluid-flow barriers that increase BTT and decrease SE (25%) and RE (22%).

ACKNOWLEDGEMENTS

This research was funded through the Reservoir Characterization and Modeling Laboratory at the University of Oklahoma. Additional funding was through the AAPG Foundation Grants-in-Aid (Norman H. Foster Memorial Grant). Software was provided by Schlumberger (Petrel and Eclipse) and Pix4D (Pix4D Mapper). We thank Javier Tellez and Justin Lewis for assistance in the field. We would also like to thank reviewers Dr. Jessica Allen, Dr. Jon Allen and editor Dr. Lauren Birgenheier for their assistance in editing and reviewing this article.

REFERENCES

- CANT, D. J., V. G. ETH, 1984, Lithology-dependent diagenetic control of reservoir properties of conglomerates, Falher Member, Elmworth Field, Alberta: AAPG Bulletin, v. 68, n. 8, p. 144-154, doi:10.1306/ad4616c9-16f7-11d7-8645000102c1865d.
- CLARKE, R. H., 1979, Reservoir properties of conglomerates and conglomeratic sandstones: The American Association of Petroleum Geologists Bulletin, v. 63, no. 5, p. 799-809.
- COLE, R.D. AND G.E. MOORE, 2012, Lithofacies, depositional systems, and reservoir elements in the Burro Canyon-Dakota interval, southwest Piceance Basin, Colorado: AAPG Annual Convention Abstracts, n. 90156.
- COLLINS, B.A. 1970, Geology of the coal-bearing Mesaverde Formation (Cretaceous), Coal Basin area, Pitkin County, Colorado: Colorado School of Mines, Master's thesis, 116 p.
- CURRIE, B.S., DARK, J.P., MCPHERSON, M.L., AND PIERSON, J.S., 2008B, Fluvial Channel Architecture of the Albian-Cenomanian Dakota Formation, Southern Uinta Basin, in M.W. Longman, and C.D. Morgan, eds., Hydrocarbon systems and production in the Uinta Basin, Utah. Rocky Mountain Association of Geologists and Utah Geological Association Publication 37, p. 65-79
- DECELLES, P. G., 2004, Late Jurassic to Eocene evolution of the Cordilleran Thrust Belt and Foreland basin system, Western USA. American Journal of Science, v. 304, p. 105-168.
- JOHNSON, R. C., 1989, Geologic history and hydrocarbon potential of Late Cretaceous-age, low-permeability reservoirs, Piceance Basin, Western Colorado: U.S. Geological Survey Bulletin 1787-E, 51 p.
- JOHNSON, R.C., AND R.M. FLORES, 2003, History of the Piceance Basin from latest Cretaceous through early Eocene and the characterization of lower Tertiary sandstone reservoirs: in Peterson, K. M., Olson, T. M., and D. S. Anderson, 2003, Piceance Basin Guidebook: Rocky Mountain Association of Geologists, Denver, Colorado, p. 21-61.
- KIRKLAND, J. I., R. L. CIFELLI, B. B. BRITT, D. L. BURGE, F. L. DECOURTEN, J. G. EATON, AND J. M. PARRISH, 1999, Distribution of vertebrate faunas in the Cedar Mountain Formation, East-Central Utah: Vertebrate Paleontology in Utah, v. 99, no. 1, p. 201-218.
- KIRKLAND, J. I., AND S. K. MADSEN, 2007, The lower Cretaceous Cedar Mountain Formation, Eastern Utah: The View Up an Always Interesting Learning Curve: Geological Society of America- 2007 symposium, v. 35, p. 1-108.
- LEWIS, K. D., 2018, Fluvial architecture of the Burro Canyon Formation using UAV-based photogrammetry and outcrop-based modeling: implications for reservoir performance, Rattlesnake Canyon, southwestern Piceance Basin, Colorado: Master's thesis, University of Oklahoma, Norman, Oklahoma, p. 1-120.
- MCPHERSON, M. L., B. S. CURRIE, J. P. DARK, AND J. S. PIERSON, 2008, Outcrop-to-subsurface correlation of the Cretaceous Cedar Mountain and Dakota Formations, Southern Uinta Basin, in M. W. Longman, and C. D. Morgan, eds., Hydrocarbon Systems and Production in the Uinta Basin, Utah: Rocky Mountain Association of Geologists and Utah geological Association, v. 37, p. 43-63.
- MASSART, B.Y.G., M.D. JACKSON, G.J. HAMPSON, H.D. JOHNSON, B. LEGLER, AND C. A.-L. JACKSON, Effective flow properties of heterolithic, cross-bedded tidal sandstones: Part 1. Surface-based modeling. AAPG Bulletin, v. 100, n. 5 p. 697-721, doi:10.1306/02011614221.
- PATTERSON, PENNY E., RAYMOND L. SKELLY, AND CLIVE R. JONES, 2012, Climatic controls on depositional setting and alluvial architecture, Doba Basin, Chad, in O. W. Bagan, Y. Bartov, K. Bohacs, and D. Nummedal, eds., Lacustrine sandstone reservoirs and hydrocarbon systems: AAPG Memoir 95, p. 265-298.
- PRANTER, M. J., A. I. ELLISON, R. D. COLE, AND P. E. PATTERSON, 2007, Analysis and modeling of intermediate-scale reservoir heterogeneity based on a fluvial point-bar outcrop analog, Williams Fork Formation, Piceance Basin, Colorado: AAPG Bulletin, v. 91, p. 1025-1051, doi:10.1306/02010706102.
- PRANTER, M. J., COLE, R. D., PANJAITAN, H. & SOMMER, N. K. 2009, Sandstone-body dimensions in a lower coastal-plain depositional setting: lower Williams Fork Formation, Coal Canyon, Piceance Basin, Colorado, U.S.A. AAPG Bulletin, v. 93, 1379-1401.
- STOKES, W. M., 1952, Lower Cretaceous in Colorado Plateau: American Association of Petroleum Geologists Bulletin, v. 36, no. 9, p. 1766-1776.
- VILLAMIZAR, C. A., G. J. HAMPSON, Y. S. FLOOD, AND P. J. R. FITCH, 2015, Object-based modelling of avulsion-generated sand body distributions and connectivity in a fluvial reservoir analogue of low to moderate net-to-gross ratio: Petroleum Geoscience, v. 21, no. 4, p. 249-270, doi:10.1144/ptgsoc2015-004.
- YOUNG, R. G., 1975, Lower Cretaceous rocks of northwestern Colorado and northeastern Utah. Rocky Mountain Association of Geologists- 1975 Symposium, p. 141-147.

Accepted August 2018